MCGILL UNIVERSITY- DEPARTMENT OF BIORESOURCE ENGINEERING

BREE 495: SENIOR DESIGN PROJECT

IMPROVED SOLAR HERB DEHYDRATOR

Zoe Martiniak
Carly Wolfe
Paul Louis Crouzat

Presented to Dr. Grant Clark
April 14th, 2015

Executive Summary

In agriculture, post-harvest drying is a necessary method to preserve the harvested crop. The way in which a product is dried has a major impact on the final quality of the product. This is of particular importance for MacDonald Student Ecological Gardens (MSEG), for they need to dry herbs to be sold as teas and spices. The proposed solution is a higher capacity solar herb dehydrator that can be located on the farm for easy accessibility. A solar herb dehydrator comprises of a solar collector to receive solar radiation to heat up the air and a drying chamber, in which the herbs will be dried. Temperature, airflow, and relative humidity are important parameters to control during the drying process. We modeled the airflow within our dehydrator using the multi-physics program COMSOL and a maximum air velocity of 1.8 m/s was achieved during steady state. An appropriate temperature to reach for the drying of herbs is 30 to 45 °C. The prototype was then constructed out of available materials and the design was tested under halogen lights to simulate the sun. A thermostat with probes placed at four different locations (ambient, two in the drying chamber and solar collector) provided us with data to determine overall temperature change. Ambient temperature remained at 20°C and temperatures within the drying chamber reached up to 27°C. The recommended optimization of our design includes the addition of a fan or controlled roof ventilation. Solar drying remains an economical and environmentally friendly drying method which can be implemented in developing countries where sunlight is abundant.

Acknowledgements

We would like to extend our gratitude to our project advisor Dr. Grant Clark, whose experience and organizational skills provided valuable insight in all avenues of the design process.

We would also like to thank our mentor Dr. Vijaya Raghavan for providing us with the technical information on post-harvest drying and food preservation. Our design would not have adequate to-date literature review without your help!

Many thanks to Scott Manktelow and Samson Sotocinal in the machine shop, your vast years of experience in constructing machines and practical knowledge was tremendously valuable during construction of our prototype. We also thank you for letting us use extra materials from the shop since we working on a scarce budget.

Finally, we would like to thank Northwest Hydraulic Consultants for providing us with additional materials to construct the prototype.

Improved Solar Herb Dehydrator

Table of Contents

Improved Solar Herb Dehydrator

1. INTRODUCTION

MSEG is a manifestation of sustainable farming at McGill University, consisting of a 1 ¼ acre farm located at Sainte-Anne-De-Bellevue, Quebec. The MSEG Druids project is dedicated to growing numerous types of herbs for selling tea and spice mixtures, as well as bulk herbs. The harvest season is from June to September and the main types of herbs they grow include chamomile, mint, bergamot, sage, lemon balm, stevia, basil, and parsley. These herbs and spices are appreciated for their powerful flavor and aromatic properties, which is an important aspect of their marketing value. It is important that these herbs are preserved in a way that maintains the flavor and aroma.

Post-harvest preservation is an important component of food preparation to inhibit microbial growth and prevent rotting and any form of degradation caused by biochemical reactions (Hii et al., 2012). There are many post-harvest preservation methods available, however only few methods are commercially used due to economic viability. The most conventional method that is still widely used for herb preservation is dehydration. For the purpose of this report, we will be using the terms drying and dehydrating interchangeably. Herbs are ordinarily dried at milder temperatures than food for market sale in order to prevent rotting and degradation of aromatic compounds.

Solar radiation is an energy source that can be used for solar drying. Sun drying is one of the oldest drying methods and it is an economical solution in places where sunlight is abundant (Raghavan, 2015). The drawbacks of open sun drying are: overexposure of product to sun and wind, attack by dust and insects, and non-uniform drying (Raghavan, 2015). Therefore, solar drying systems are a possible replacement for sun drying as the product is not directly exposed to the environment.

There are many advantages to using a solar drying system. By supplying the product with more heat than is available under ambient conditions, the rate of drying can be increased due to the higher temperature and movement of the air with a lower humidity (Weiss & Buchinger, 2012). Secondly, the product is enclosed within the drying chamber and is thus protected from dust, insects, birds, animals, and rain (Weiss & Buchinger, 2012). Thirdly, dryers are typically constructed from low-cost and locally available materials (Weiss & Buchinger, 2012), which make it attractive in developing countries. Furthermore, solar drying has no emissions and is considered a rather environmentally friendly method of harnessing energy. However, the main disadvantage of solar drying is it heavily depends on weather conditions and solar radiation, and can be somewhat unreliable. Solar drying depends on the location of the dryer, which indicate the weather conditions, insolation, solar elevation and duration of sunlight. Moreover, high internal temperatures can be reached in these dryers which could damage the product. Therefore, we must address these issues in our design. The goal of this design is to develop a solar herb dehydrator that MSEG can implement such that they can increase the quantity of herbs dried and increase the efficiency of the process.

2. LITERATURE REVIEW

Drying is a process in which moisture is removed from the product until the desired moisture content is attained. One must apply heat to remove the moisture from the product and then have a means to remove this moisture. Therefore, our drying system will use a combination of heat and mass transfer processes:

(i) Heat transfer: heat is transferred to evaporate liquid (Hii et al., 2012)

(ii) Mass transfer: mass is transferred as a liquid or vapor within the solid and as a vapor from the surface (Hii et al., 2012)

Drying first occurs at a constant rate and then a falling rate. During the constant rate drying period, the herbs are moist and remain wet during drying so the water is evaporated as from a free water surface (Khoshmanesh, 2006). The constant rate drying period depends on the heat or mass transfer coefficient, the area exposed to the air, and the difference in temperature or humidity between the air and the wet surface of the herb (Hii et al., 2012). The falling-rate period begins at the critical moisture content when the constant rate period ends. Once critical moisture content is reached, the drying rate slows and a larger temperature gradient is required (Raghavan, 2015). The temperature will asymptotically approach the inlet drying gas temperature as equilibrium moisture content is reached (Raghavan, 2015). In this period, the drying rate is controlled by product internal heat and mass transfer (Raghvavan, 2015). The internal moisture transfer is by diffusion, capillary action, pressure gradient or a combination (Raghavan, 2015).

Drying of agricultural products depends on (Weiss & Buchinger, 2012):

- Product characteristics: properties, size, shape, pre-treatment, bulk density
- Drying requirements: initial moisture content, final moisture content
- Drying conditions: temperature, relative humidity, air velocity, thickness of layer

To understand the drying process, one must thoroughly review the psychrometric chart. The psychrometric chart in appendix 1 gives the properties of an air-vapor mixture that controls the rate of drying (Hii et al., 2012). The water must be heated to a temperature at which its vapor pressure equals or exceeds the partial pressure of vapor in the air (Hii et al., 2012).

Solar dryers can be divided into two classifications based on their heating modes. Either an active solar energy drying system (hybrid solar dryers) or a passive solar energy drying system. Active solar dryers use forced convection (e.g. using a fan) whereas passive solar dryers rely solely on natural circulation or natural convection systems. The passive dryer is appropriate for our application of on-farm use as the entire system depends on solar energy. This solar energy can be absorbed either directly or indirectly. The advantage of using an indirect solar drying method is that the herbs are not exposed to the direct rays of the sun so this reduces the loss of colour and vitamins in the herbs (Weiss & Buchinger, 2012). In this method, the air is heated in the solar collector and then ducted to the drying chamber to dry the product (Akarslan, 2012). However, this method tends to over-dry the herbs on the bottom tray and has a low efficiency in the later stages of drying when most of the trays are dry (Weiss & Buchinger, 2012).

To minimize cost and complexity of the design, we decided to use passive solar technology. Based on the literature reviewed, the cabinet drying configuration is the optimal design for passive solar drying (Bhuiyan et al., 2011; Scanlin, 1997; Scanlin et al., 1999; Weiss & Buchinger, 2012). The drying mechanisms of the passive solar cabinet dryers is illustrated in figure 1 below.

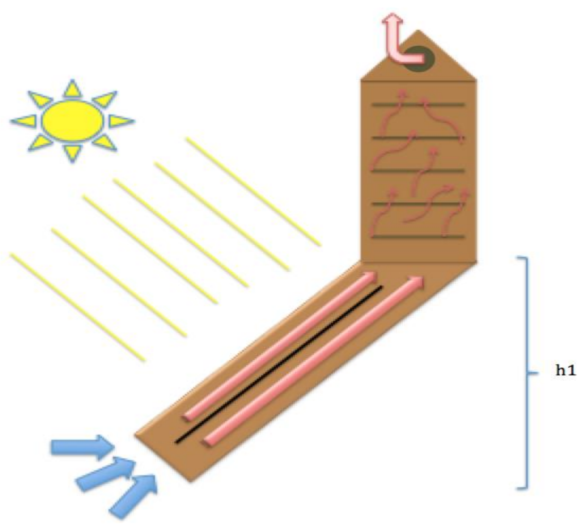

Figure 1. Illustration of the drying mechanisms in a passive solar drying cabinet.

Air is drawn through the inlet of the solar collector by natural convection. This flow of air is created by the fact that the air inside the dryer is lighter than the cooler air outside (Weiss & Buchinger, 2012). The solar collector should have an angle of inclination specific to the solar elevation to receive maximum radiation and the sunlight heats up the black absorber within the collector. This heats the air entering into the unit as it passes through the collector with laminar flow. The drying air becomes turbulent when it hits the trays. This hot air rises and then is partially cooled as it picks up moisture from the herbs in the drying chamber. The drying is achieved by the difference in moisture content between the drying air and the air in the vicinity of the herbs (Akarslan, 2012). Finally, the air leaves through the vents at the top of the drying cabinet. The difference in density creates a negative pressure which draws more fresh air in from the bottom. This effect increases the higher the drying cabinet is above the inlet, as illustrated as h1 in figure 1 above (Weiss & Buchinger, 2012). A steady state is achieved when the heat required for evaporation and the heat losses from the system combine to equal the total heat absorbed (Blair et al., 2005).

The performance of the dehydrator should be evaluated through energy and exergy analysis. Exergy is the energy that is available to be used. After the system and surroundings reach equilibrium, the exergy is zero. Determining exergy is the first goal of thermodynamics. The exergy values are calculated by using the characteristics of the working medium (air) from a first-law energy balance (Akpinar, 2011).

Exergy equation applicable for steady flow systems (Akpinar, 2011):

$$\dot{E}x = \bar{c}_{\mathrm{Pda}}\left[(T - T_{\infty}) - T_{\infty}\ln\frac{T}{T_{\infty}}\right]$$

For exergy inflow of the drying cabinet (Akpinar, 2011).:

$$\dot{E}x_{\mathrm{dci}} = \bar{c}_{\mathrm{Pda}}\left[(T_{\mathrm{dci}} - T_{\infty}) - T_{\infty}\ln\frac{T_{\mathrm{dci}}}{T_{\infty}}\right]$$

For exergy outflow of the drying cabinet (Akpinar, 2011).:

$$\dot{E}x_{\mathrm{dco}} = \bar{c}_{\mathrm{Pda}}\left[(T_{\mathrm{dco}} - T_{\infty}) - T_{\infty}\ln\frac{T_{\mathrm{dco}}}{T_{\infty}}\right]$$

However, the exergy losses throughout the process are determined by (Akpinar, 2011).:

$$\Sigma\dot{E}x_{\mathrm{L}} = \Sigma\dot{E}x_{\mathrm{i}} - \Sigma\dot{E}x_{\mathrm{o}}$$

From this we can get the exergetic efficiency (ratio of exergy use in the drying of the product to exergy of the drying air supplied to the system) which computes the efficiency of the drying process (Akpinar, 2011).:

$$\text{Exergetic Efficiency} = \frac{\text{Exergy outflow}}{\text{Energy inflow}} = \frac{\text{Exergy inflow} - \text{Exergy loss}}{\text{Exergy inflow}}$$

$$\eta_{\mathrm{Ex}} = \frac{Ex_0}{Ex_1} = 1 - \frac{Ex_{\mathrm{L}}}{Ex_{\mathrm{i}}}$$

Where:

$\boldsymbol{c_{Pda}}$= average specific heat of drying air (kJ/kg*K)

$\dot{\boldsymbol{E}}\boldsymbol{x_o}$= exergy outflow (kJ/s)

$\dot{\boldsymbol{E}}\boldsymbol{x_i}$= exergy loss (kJ/s)

$\dot{\boldsymbol{E}}\boldsymbol{x_{doi}}$= exergy inflow to drying cabinet (kJ/s)

$\dot{\boldsymbol{E}}\boldsymbol{x_{doo}}$= exergy outflow to drying cabinet (kJ/s)

$\boldsymbol{T_{doo}}$= temperature of air at outlet of drying cabinet (°C)

$\boldsymbol{T}_{\infty}$= reference temperature (°C)

3. DESIGN SPECIFICATIONS

When designing our dehydrator, it was important to keep in mind the goals set out by the client while respecting the food regulations and codes set out by Health Canada. A major criterion for our design was to increase the capacity of the dehydrator as well as reduce labour requirements, as well as consider the quality of the herbs and how the drying process may affect the flavor and aroma of the herbs. Another criterion is the durability of the dryer and ensuring that it is weather proof. Finally, the cost of the materials used for construction is a crucial consideration for our design.

3.1 Design Overview

The following figure 2 illustrates the original blueprints (a) and isometric view (b) of the dehydrator. The details of each of the different components of the dehydrator are further explained in the following section.

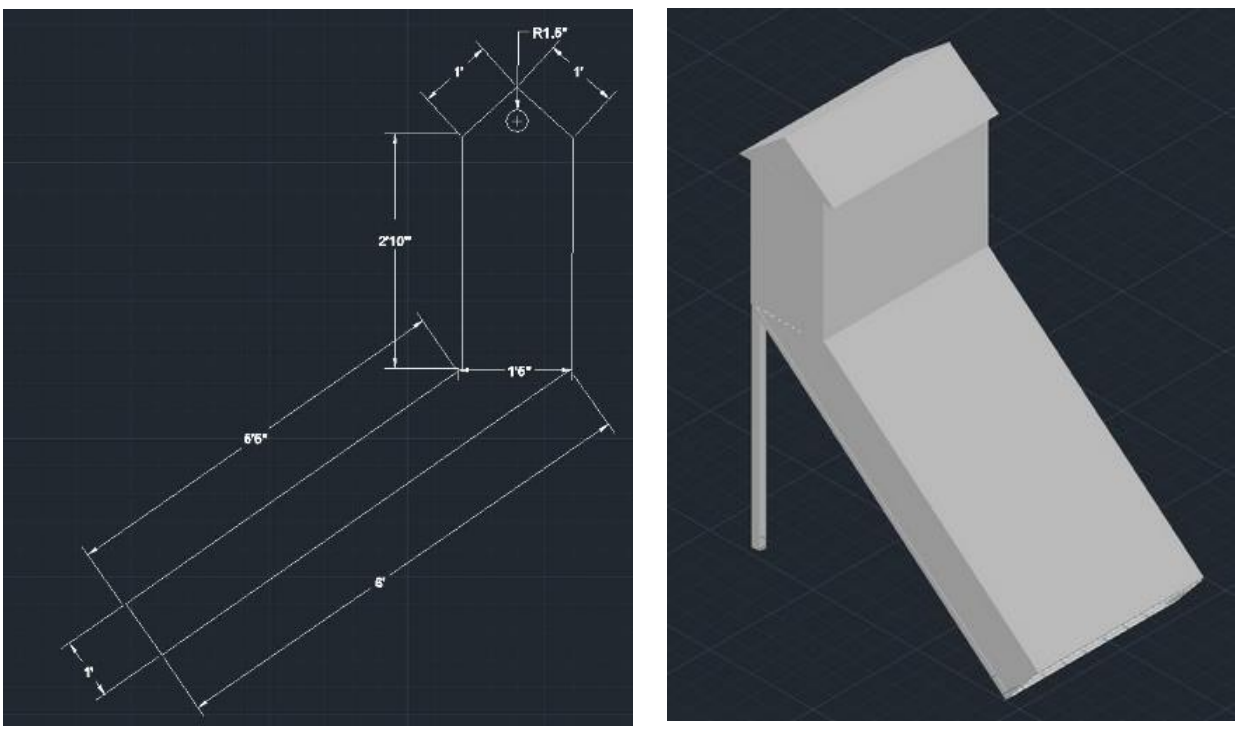

Figure 2: a) Blueprint of side view of dehydrator   b) Isometric view of dehydrator.

3.1.1 Drying Conditions

Maintaining the quality of the aromatic content of herbs is an important consideration when drying. The essential oils of herbs are comprised of these aromatic compounds that are essential to the herb's fragrance and flavor. Many of these aromatic compounds tend to be volatile and are the most sensitive components in the drying process (Müller, 2007). To preserve these sensitive ingredients, drying at low temperatures and high air velocities is generally recommended (Müller, 2007). The quality threshold is defined as the minimum quality of the product which is acceptable by consumers. To obtain optimal drying capacity, the drying temperature should be the highest allowable temperature without reducing the quality of the product below the quality threshold. Table 1 summarizes the effect of drying temperature on the content of essential oils in various herbs. The optimal temperature ranges between 30-40°C for most herbs (Müller, 2007). We also need to take the time and relative humidity into consideration. Since the herbs will most likely be left in the dehydrator for the entire day, we want to avoid drying them out. Generally, we would like to achieve a final herb moisture content between 13-15% (Scanlin, 1997). Herbs are considered dried when the leaves are crispy dry and crumble easily between the fingers (Reynolds & Williams, 2006).

3.1.2 Site Analysis

The performance of our solar dryer will highly depend on the weather conditions. Important parameters to look at include mean temperature, maximum temperature, minimum temperature, relative humidity, wind speeds, and rainfall. The drying season will be between June and September. We have retrieved the climate data for Sainte-Anne-de-Bellevue. The weather data from 2014 is presented in Table 2 in appendix 2.

An appropriate temperature range for drying herbs is 30 to 40 °C, however drying in areas with high humidity can require temperatures up to 52°C (Reynolds & William, 2006). Since our herbs will be dried during the day when the outside temperature is the near the hottest (average maximum temperature), we will need to increase the temperature by 10 to 20 °C within the drying chamber. Drying times typically vary between 1 and 4 hours (Reynolds & William, 2006), the herbs should be checked periodically to avoid over drying. An important aspect of our design will be to ensure that the herbs do not get over dried. This can be prevented by having adjustable vents at the top of the drying chamber, which can control the temperature and airflow.

3.2 Solar Air Collector

The angle of inclination of the solar collector depends on the solar elevation during the day. The maximum amount of radiation will be absorbed by the solar collector if the solar radiation hitting the collector has an incident angle of 90°. However, the average solar elevation varies from day to day. Solar insolation will be lowest in September, as indicated in the insolation graph in figure 2 of appendix 1. Therefore we will want to design the solar collector so that it will be able to maximize the heating effect for the month of September. The solar elevation will be around 45° in August to September, and therefore the angle of inclination should be 90°-45°=45°.

The solar air collector is the chamber in which the air is heated up by solar radiation. Upward heat losses from the solar collector are minimized by the use of a transparent cover above the absorber plate. The top of the solar collector needs a material that is transparent so that it will transmit the suns rays through to the absorber and then prevent heat losses due to convection and long-wave radiation (Ekechukwu & Norton, 1999). In addition, the material must be waterproof and stable to deterioration under heat and UV radiation.

Energy gained from the solar collector is calculated using the magnitude of the solar radiation (Akpinar, 2011):

$$\dot{Q}_c = \dot{m}_{da} c_{Pda} (T_{co} - T_{ci})$$

Where:
$\dot{Q}_c$= energy taken from solar collector (kJ/s)
$\dot{m}_{da}$= mass flow rate of drying air (kg/s)
c_{Pda}=specific heat of drying air (kJ/kg*K)
T_{co}= temperature of air leaving solar collector (°C)
T_{ci}= temperature of air entering solar collector (°C)

The requirements for the absorber plate within the solar collector are: high absorbance of incident radiation, low emissivity, good thermal conductivity, be thermally stable, durable, lightweight, and cheap. A material should be chosen with a high thermal conductivity in order to transmit large amounts of heat quickly. Aluminum has a high thermal conductivity of 235 W/(m*K) and thus is an ideal material for this application (Inglehart, ND). This material will be painted black for a black object absorbs all wavelengths of light and converts them into heat. However, it was important to apply a light coat of paint so that the paint does not decrease the conductivity of the material.

3.3 Drying Chamber

For a functioning dehydrator it is essential that the drying chamber be well insulated and sealed in order to minimize heat loss and leakage to the environment. This ensures that the drying of the herbs is efficient. Therefore the main material that we used for the drying cabinets is wood along with sealers and coating paint.

Wood is the material that was used for MSEG's current dehydrator and is also the material that we have chosen to use for our design. The advantage of wood is that it is durable, relatively inexpensive, and a natural insulator. Therefore we opted for a ¾" standard plywood since it has a high conductive resistance of 0.95 (Mazria, 1979). To minimize air leakage, it is important to seal the edges of the cabinet with silicon glue, this ensures no leakage of air. The doors of the solar collector pose primary concern in terms of leakage, so sealing them effectively is an essential part of the design. We propose using ¼” foam tape around the cracks of the doors to prevent leakage, and to stop all dust and other undesirable particles from entering the drying cabinet. Finally, to ensure that the cabinet along with the wooden structure would be resistant to the varying weather conditions, the structure must be coated with wood varnish paint, thus making the structure withstand high temperature, sunlight and water.

The blueprint drawing of the back of the drying chambers is shown in figure 3 below.

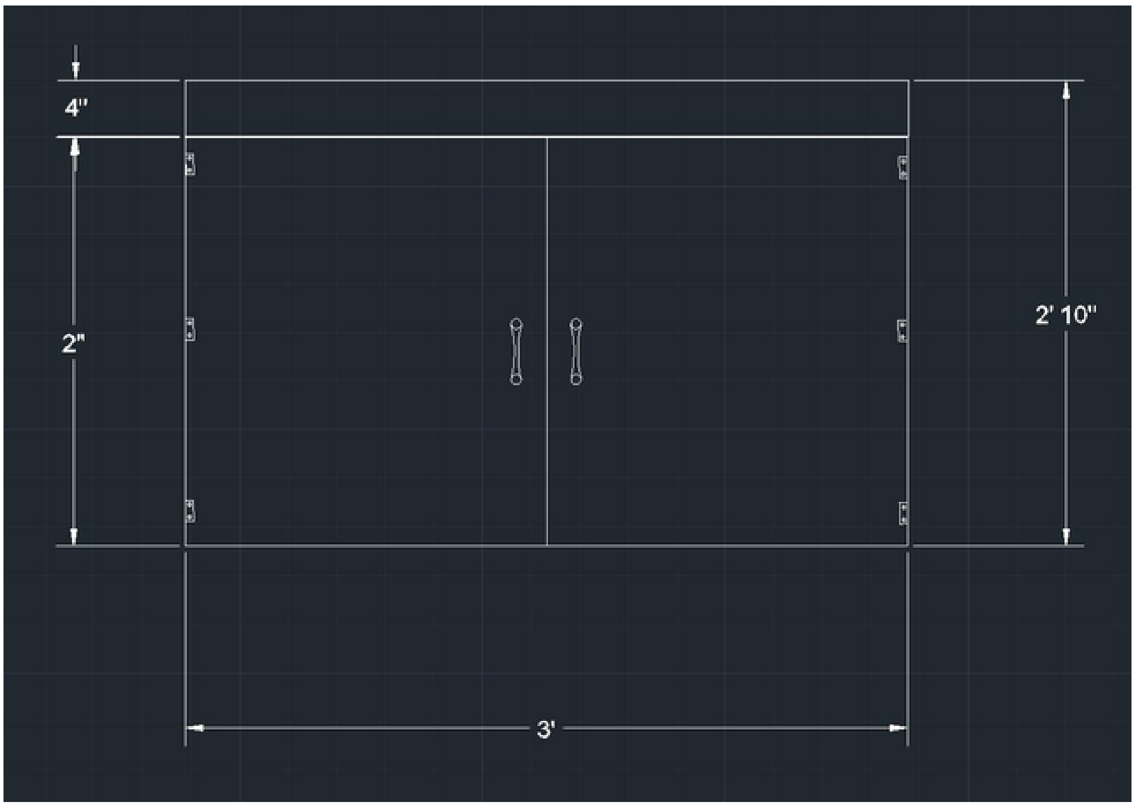

Figure 3. Back view of the drying chamber.

Energy analysis within the drying chamber can be used to determine the heat transfer to the herbs, and therefore used in the process of drying. The heat used during the dehumidification process can be estimated by (Akpinar, 2011).:

$$\dot{Q}_{dc} = \dot{m}_{da}(h_{dci@T} - h_{dco@T})$$

Where:
$\dot{\boldsymbol{Q}}_{dc}$= heat used in drying cabinet (kJ/s)
$\dot{\boldsymbol{m}}_{da}$= mass flow rate of drying air (kg/s)
$\boldsymbol{h}_{dci}$= enthalpy of air entering the drying cabinet (kJ/kg)

h_{dco}= enthalpy of air leaving the drying cabinet (kJ/kg)

From this, we can get the energy utilization ratio of the drying cabinet (Akpinar, 2011).:

$$EUR = \frac{\dot{m}_{da}(h_{dci} - h_{dco})}{\dot{m}_{da} c_{Pda}(T_{co} - T_{ci})}$$

The energy utilization ratio is an important parameter to determine the efficiency of the process.

3.4 Trays

The trays will be made of a wooden frame and stainless steel mesh, which the herbs will be dried on. It was important to choose a material for the trays that is food-safe, which is why stainless steel mesh is ideal. The wire mesh will create a turbulent flow of air, which provides a more uniform temperature distribution as well as increases the heat transfer in the drying chamber.

One of our design goals was to increase the capacity of herb dehydrator. Therefore this is an important consideration in our design of tray dimensions and number of trays. The drying capacity in the old dehydrator is compared to the design of the new dehydrator in table 1.

Table 1. Tray capacity comparison.

	Old dehydrator	New dehydrator
Tray area	0.1	0.35
Number of trays	8	5
Total drying area	0.8	1.75
Increased capacity		195%

3.5 Vents and Chimney

The major parameters affecting food drying are temperature, humidity and airflow, and all of these parameters are interactive (Scanlin, 1997). The size of the vent opening is directly proportional to airflow and inversely proportional to temperature. Since high velocities are desired, a rather large vent area is required. However, reducing the vent area will achieve higher temperatures and therefore lower relative humidity. It is important to optimize the size of the vent opening in order to achieve optimal drying conditions. The vent size will be an important testing parameter in our prototype evaluation.

To further increase the efficiency of the airflow, we decided to incorporate a chimney into the design. This additional control mechanismwill enhance the natural convection of the solar dryer. Indeed, the buoyancy force imposed on the air stream will be increased and provide a greater airflow velocity and, thus, a more rapid rate of moisture removal. Research by El-Sebaii et al., 2002; Pangavhane et al., 2002; Bena and Fuller, 2002; Condorı´ and Saravia, 2003; Ivanova et al., 2003; Simate, 2003; Chen et al., 2005; and Forson et al., 2007 has shown the advantages of incorporating a solar chimney to the dehydrator design. From the literature, it is suggested that the longer the chimney, the better the results. Therefore we propose a 2'6" cylindrical chimney with a diameter of 4", this way the length is optimized while making sure the structure is stable, so to limit failure under lateral stresses during transportation and wind.

4. EXPERIMENTAL MODELING

4.1 COMSOL Simulation

The modeling was done using the Multiphysics program COMSOL 4.3a. In order to build the 2 dimensional model, it was necessary to make several assumptions:

- The walls are perfectly insulated such that there is no air leakage.
- There is no external convection from the outside.
- The solar radiation is 400 W/m^2 (See insolation in figure 2 of appendix 1)
- The initial temperature of the fluid is 293 K
- The length of the dehydrator is infinite in the z-axis

After choosing the 2D special setting, we chose a time dependent study so the model would evolve with time as would the dehydrator in a real setting. The two physics that were coupled were Laminar Flow under the fluid flow section and heat transfer in solids.

The equations that reign in the physics in the model are the Navier-Stokes equations for compressible flow:

$$\boldsymbol{\rho \frac{\partial u}{\partial t} + \rho(u * \nabla)u = \nabla * [-pI + \mu(\nabla u + (\nabla u)^T) - \frac{2}{3}\mu(\nabla * u)I] + F}$$

$$\boldsymbol{\frac{\partial \rho}{\partial t} + \nabla * (\rho u) = 0}$$

and the general equation for heat transfer:

$$\boldsymbol{\rho C_p \frac{\partial T}{\partial t} + \rho C_p u * \nabla T = \nabla * (k \nabla T) + Q}$$

Where:

u=velocity (m/s)

I= identity matrix

μ = dynamic visciosity (Pa $*$ s)

∇ = del operator

p = pressure (Pa)

C_p = heat capacity $\left(\frac{\mathrm{J}}{\mathrm{kg} * \mathrm{K}}\right)$

T = temperature (K)

k = thermal conductivity $\left(\frac{\mathrm{W}}{\mathrm{m} * \mathrm{K}}\right)$

Q = heat flux $\left(\frac{\mathrm{W}}{\mathrm{m}^2}\right)$

Then we built the geometry respecting the lengths of our final design and chose the built-in fluid, air, into the model. It was necessary to add inlets and outlets in order to create an air stream throughout the dehydrator. Then, we incorporating gravity as a parameter and set up a volume force in the fluid, F=-spf.rho*g. This way COMSOL understands the effect of gravity on the fluid. The results of the COMSOL model are illustrated in figure 4.

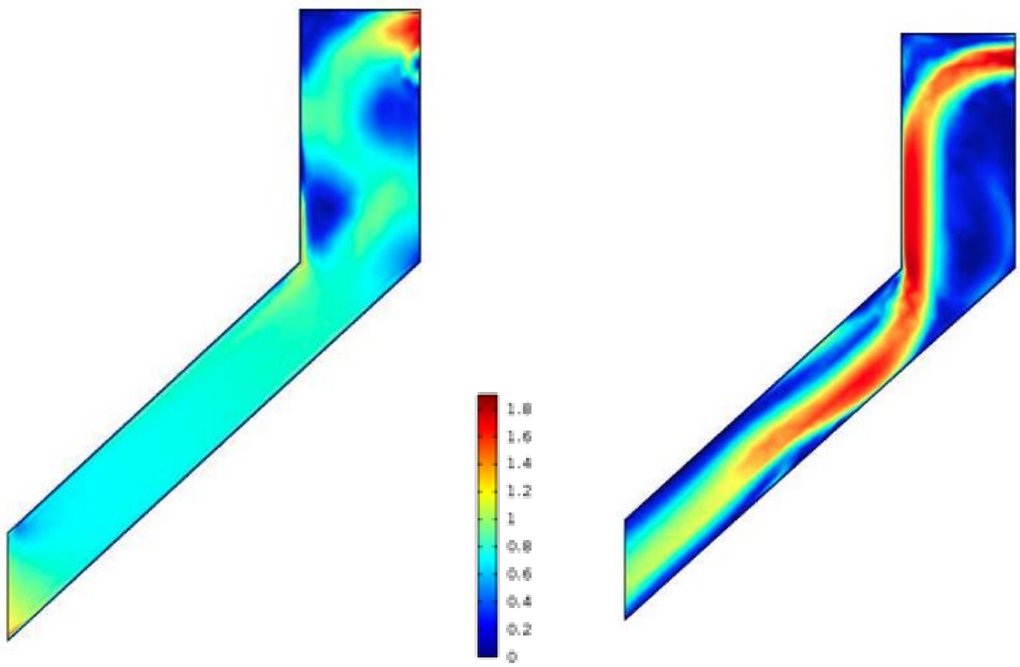

Figure 4: a) Model After 30 seconds , b) Model in Steady State

The results turned out promising, the air stream was achieved at steady state and a maximum velocity of 1.8 m/s shown in the model in red. However the model was solely used to have a better understanding of the underlying physics of our design and does not incorporate any biomass. Therefore we can imagine that the total airflow would be greatly reduced in a real setting.

Additionally, it will be necessary to properly validate it with the prototype once the conditions are suitable. This is an essential part in the perfection of a model that should never be disregarded. Moreover, incorporating the various external forces and climatic conditions on to the mode in the form of external convection coming from the wind, will increase its accuracy.

Also managing to make the intensity of solar radiation time-dependent would help recreate the real life conditions where the intensity becomes stronger as the sun approaches its zenith and then gradually decreases. A last improvement to make to the model and probably one of the most important ones, would be to replicate the biomass being dried inside of the herb dryer. This will enable us to see the rate at which the moisture is removed and make predictions about overheating and rotting. However in order to do this, we would have to incorporate equations for moisture removal.

4.2 Prototype Construction

The construction of the solar dehydrator was set out in the machinery shop of Macdonald Campus under the supervision of Scott Mankeltow and Samson Sotocinal. The process lasted a total of 4 days, spanning about 30 to 40 hours. Thanks to the equipment available at the shop and the woodworking knowledge of both supervisors, the efficiency of construction was considerably increased. See appendix for time lapse of construction.

4.2.1 Materials

The materials which we used for construction of our prototype were limited by cost and availability. Unfortunately at the beginning of this semester all funding was discontinued. This was the major drawback we faced when buying materials for construction. Luckily, thanks to generosity of the Northwest Hydraulic Consultants, we were able to cover most of our supplies by recycling the materials the company uses when building their prototype. This included, 3 sheets of 4 by 8 plywood, a 3 by 5'5" panel of acrylic plexiglass and 2 pieces of 2" by 4" hardwood. The plexiglass is an ideal material for the transparent cover of solar absorber based on its high transmittance of visible light, as indicated in table 2.

Table 2. Material properties

Plexiglass	**Value**	**Units**	**Reference**
Transmittance of visible light	0.87	-	(Ekechukwu & Norton, 1999)
Transmittance of infrared radiation	0.01	-	
Tensile strength	55-60	N/mm^2	
Carbon steel	**Value**	**Units**	
Thermal conductivity	45	W/m^2	(Inglehart, ND)

Furthermore we were able to recuperate additional material from the machinery shop, such as a carbon steel for the solar absorber, a metal pipe and an L shaped bracket for the wheels along with all the screws and nails necessary for our design.

4.2.2 Design Modifications

One of the main modifications we made during construction was regarding the wheels and the way they would hold to the solar dehydrator. After a review of the literature and consultation with Samson Sotocinal, we decided to weld the wheels to a shaft as seen in figures 5 and 6 below. We used long metal pipe, spanning the width of the solar collector with an additional ½ inch on both sides, on which we welded ¾" screws at each end, where the wheels will be attached. Finally to ensure that the shaft is well attached and can resist stress in all lateral directions, we welded two L shaped brackets at an exact distance of 3' from each other. This way the shaft fits perfectly on the width of the dehydrator and is thus stabilized.

Figure 5. Blueprints of the shaft for wheel support

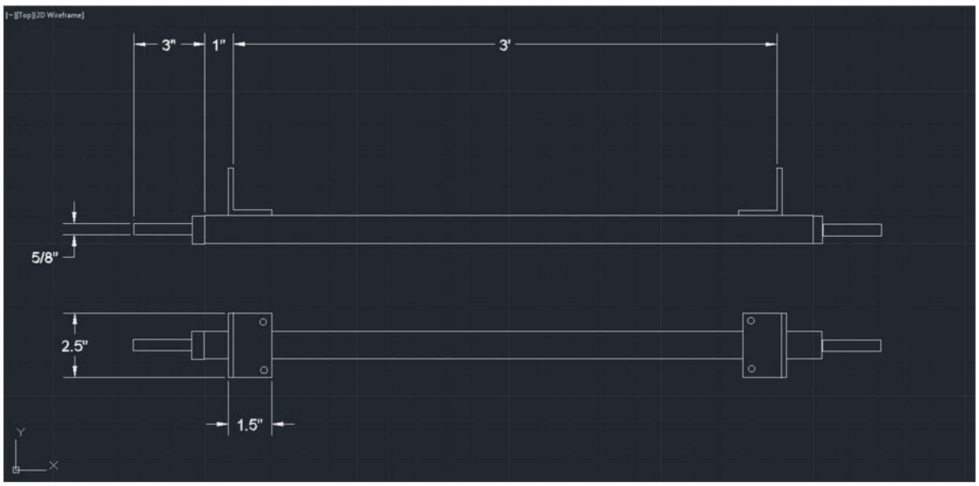

Figure 6. Isometric view of the shaft for wheel support.

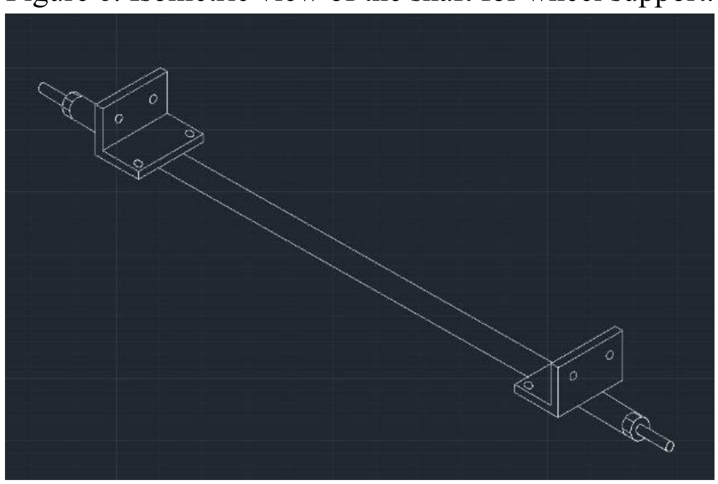

For the absorbing plant in the solar air collector, we chose to bend the steel to form an undulated surface pattern to increase the surface area and receive more solar radiation. In addition, we suspended the plate in the middle of the solar collector so that the air will flow over both the top and bottom of the plate, thus increasing the heat transfer surface area. Figures 7 and 8and show the blueprints for the solar air collector.

Figure 7. Cross-sectional view of the solar air collector with undulated steel.

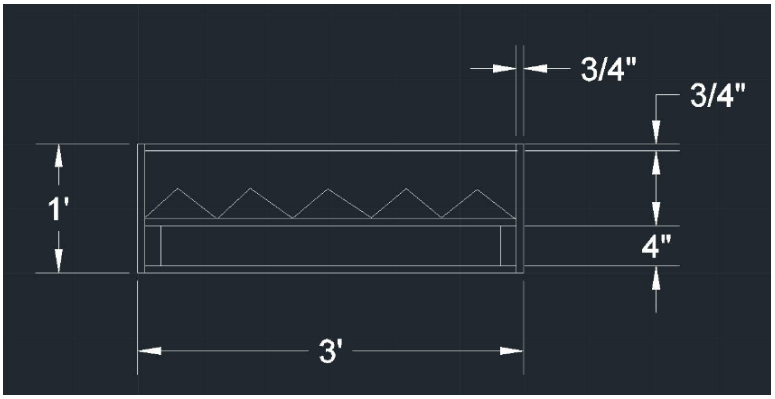

Figure 8. Top view of the solar air collector with undulated steel.

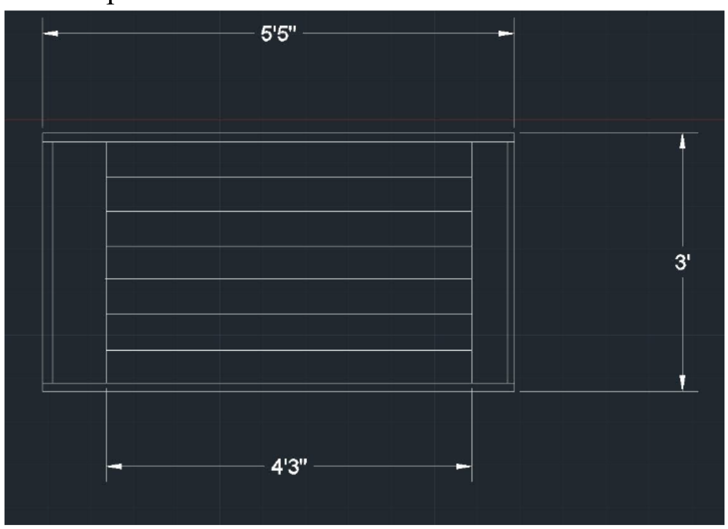

The final prototype after construction is shown in figure 9, and further illustrated in Appendix 3.

Figure 9: a) Angular view of prototype, b) Side view of prototype.

5. EVALUATION OF PROTOTYPE

In this section we will evaluate the prototype we constructed according to its performance, risk assessment, and total cost of construction. We attempted to design an adequate test of the prototype in order to evaluate its success of drying herbs in the field. The most important parameters for drying herbs are temperature, air speed and relative humidity. Therefore we needed to design a test to measure these parameters under similar external drying conditions to being placed outdoors in the summer. In order to achieve similar drying conditions, testing of the prototype would have to be in an environment with comparable temperature and relative humidity to outdoor summer average conditions. The weather data for Sainte-Anne-de-Bellevue is listed in table 2 of appendix 2. We also needed a heat source to simulate solar radiation.

To achieve these optimal drying conditions, we tested our dehydrator in the machine shop under halogen lights. The temperature within the machine shop is maintained at a temperature between 20-25°C, with fluctuations attributing to the spontaneous opening and closing of the door to the outside for various reasons such as bringing in materials. Many commercial solar simulators use halogen light technology, however Emery classifies all tungsten-halogen bulbs as Class C solar simulators due to their mismatch in spectral irradiance (1986). Therefore tungsten-halogen bulbs with dichroic filter simulators are not ideal solar simulators, and different results might be observed. The radiation from the halogen lamp is also much lower than summer solar radiation, which can reach up to 400 W/m^2 in the summer, as indicated in the insolation graph in figure 2 of appendix 1.

5.1 Data Collection

We used a Velocicalc to take readings at various positions within the dehydrator. The Velocicalc is a hand-held device that measures relative humidity, air speed and temperature simultaneously. While the portable aspect of this device is very useful, it is more accurate to take readings at the same exact point to avoid error. For this reason, we also used a thermostat with 4 different probes that could be set in specific places for the entire length of measuring. One probe measured ambient temperature, one was placed on the absorbing plate, and two were placed inside the drying chamber. It is important to take consistent temperature readings of the ambient air to provide a proper comparison with the changing inside air, due to the fluctuating temperature within the machine shop. The temperature was recorded at two different locations within the drying chamber (on the left and on the right) to provide more insight into the temperature profile within the drying chamber. Finally, a temperature probe was placed on the absorbing plate to show how successfully plate is heating up and to provide more data to be used in heat transfer equations.

The first measurement was taken without the roof on and without the plexiglass set in place in order to start the readings off with uniform temperatures and to get a better sense of how long it would take to heat up inside. After taking the first reading, the roof was added and the plexiglass was set in place. The temperature was recorded every 5 minutes or so for 84 minutes. We only took readings with the Velocicalc after 45 minutes of testing. The temperature, relative humidity, and air speed were measured twice at the inlet, inside, and outlet of the drying chamber.

5.2 Data Analysis

The results of the thermostat temperature readings are listed in table 3 in appendix 2. The temperature profile of the dehydrator is illustrated in figure 10.

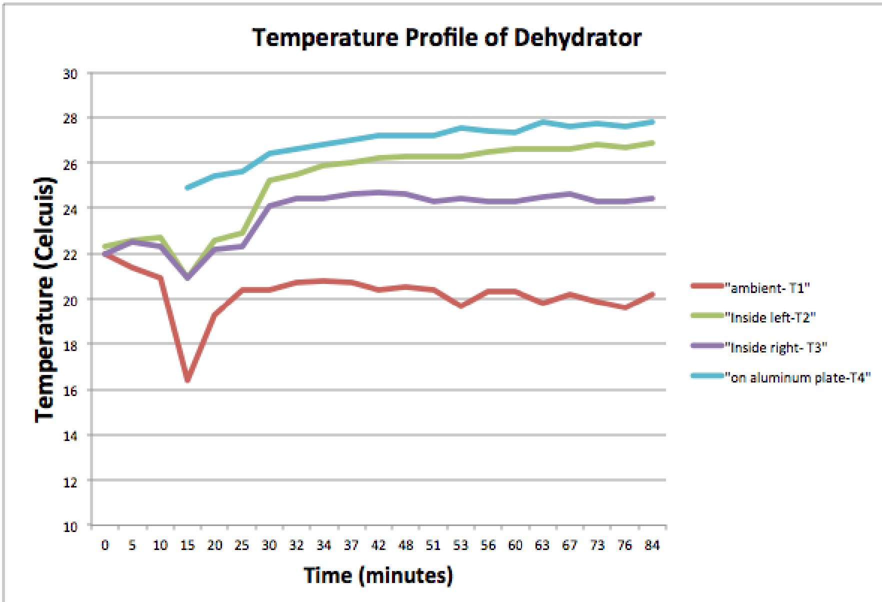

Figure 10. Graph of temperature profile within the dehydrator.

The initial temperature for all four probes showed a uniform temperature of around 22°C. The large drop in temperature in the ambient at around 15 minutes is attributed to the door opening and a lot of heat loss occurred in the shop. The temperature remained fairly stable inside the dehydrator as compared to the ambient, showing that the dehydrator is well sealed and good at maintaining high temperatures within it. The temperature of the ambient hovered around 20°C, while the temperature inside the cabinet was held at 24-26°C.

The differences between the temperatures read at different points inside the cabinet can attribute to a variety of reasons. One of the temperature probes was placed closer to the doors than the other, which could cause it to show a lower temperature reading. Hot air rises, and therefore the warmer air would hug the top of the solar air collector and would have a tendency to flow on the opposite side of the dehydrator from the doors. This effect is expected to become negligent once we add the trays, since the trays will disturb airflow and make it become turbulent within the drying chamber. Turbulent airflow will improve the mixing of air, which will create more uniform temperature distribution and drying conditions.

Unfortunately, the Velocicalc did not give us a reading for any air velocities. However we were able to feel a significant airflow on our hands near the outlet of the drying chamber. It is more important to dry herbs with a higher airflow than a high temperature to obtain higher quality herbs. The testing conditions were not ideal, and we will only be able to evaluate whether the solar dehydrator will achieve high enough velocities if we can test it outside with favorable weather conditions, or with an adequate solar simulator.

5.3 Risk Analysis

To avoid failure, we should be aware of some potential problems in the design and testing of our dehydrator. In terms of performance of the dehydrator, it should be well-insulated and airtight to avoid heat loss for optimal performance. If the dehydrator is not adequately insulated, then the temperature within the dehydrator will be more responsive to environmental changes, such as high-speed winds or changes in ambient temperature from a cloud passing overhead that can contribute to heat loss. If the structure has any cracks or opportunity for air to leak out, it will decrease and interfere with air flow throughout the structure, as well as contribute to heat loss. Any cracks in the structure will also allow water to enter the structure during rainfall, which will increase the moisture and relative humidity in the dehydrator and make it more difficult to dry the herbs. To avoid this issue, great care must be taken to properly seal the dehydrator. The top of the roof should be well sealed, ideally with a metal cover, and the roof edges will have a maximum overhang.

It is also important to consider the quality of the herbs and the fact that they will be marketed for consumption. Since these herbs will be intended for human consumption, they should also not be subject to biological degradation or contamination. One issue arising from inadequate temperatures or air velocity is herb rotting if they are left for extended periods in the dehydrator with a high moisture content. It must be proven that high enough temperatures and air speed can be achieved in average summer conditions. However problems can also arise if the temperatures reach excessive levels. High temperatures can result in loss of essential oils in the herbs, which decreases the quality of the herbs. The quality of the herbs can be detected by the essential oil content and the final moisture content. The range of optimal drying temperature and final moisture content varies for each herb and are indicated in table 1 of appendix 2.

Another problem that could arise is contamination of the herbs by any of the materials used in the construction of the dehydrator. One potential source of contamination is rotting wood, which can occur by wood-decay fungus when wood is exposed to water. We will try and avoid this by coating the wooden structure in epoxy to provide a barrier between the wood and its surroundings, as well as a water-resistant paint finish to further prevent water from infiltrating into the wood. The trays must be made of a food-grade material to prevent contamination. A highly accepted material to use as a food contact surface is stainless steel, which we will use for our trays. Another source of contamination could be from the black paint used to paint the metal absorbing sheet. It is important to purchase a high-heat paint to prevent volatiles from contaminating the herbs.

5.4 Cost Analysis

Since funding for this project did not materialize in the end, we had to make some modifications to the initial design to minimize the costs. We were able to make a fairly low-cost prototype, which relied heavily on material donations. Fortunately we received material donations of plywood and plexiglass by a local consulting firm, Northwest Hydraulic Consultants (NHC). This was greatly appreciated and significantly reduced the cost of our construction. We also were allowed to use extra material that Scott Manktelow had lying around in the machine shop, including 2x4 beams, nails, screws, a carbon steel sheet for the solar absorber, as well as the materials used in the shaft support for the wheels. The cost breakdown of material purchases is listed in table 4 of appendix 2. Our total cost of construction was $127, while we estimate it would have been $341 if we were to purchased all of the materials ourselves.

5.5 Further Testing

We would ideally want to test our dehydrator outdoors during the drying months of June to September. This would give us more accurate results that would help validate the COMSOL modeling. In addition, we would like to do testing with the herbs inside the drying chamber. The collection of air speeds and temperature data could be used in the exergy equations to determine the efficiency of our dehydrator. For further optimization of the final prototype we would test the final moisture content of the herbs and measure the essential oil content of the final product.

6. OPTIMIZATION

Based on what we learned from constructing the dehydrator and testing it, there are a couple notable improvements we would make in the final design. These include technical details in the design as well as methods to regulate drying conditions within the dehydrator.

6.1 Technical Details

One main issue in our design that we learned from construction is the placement of the wheels. The wheels should ideally go directly underneath the center of mass of the structure, as revealed by mechanical analysis. Therefore, the wheels should have been placed at the bottom of the supporting legs since the majority of the weight of the structure would be in the drying cabinet. Dr. Clark did advise us on putting the wheels at the feet, however we made the decision to place them at the bottom of the solar air collector for ease of moving. The dehydrator is currently difficult to maneuver and requires at least two people to move it. By moving the wheels to the bottom of the legs, the dehydrator can be easily moved by just one person.

6.2. Regulating Drying Conditions

As described previously, the optimal drying conditions of herbs has a specific range for temperature, relative humidity and air speed. The quality of the herbs can be optimized by regulating the drying conditions within the dehydrator. Since obtaining higher air speeds are more important than higher temperatures in herb drying, it is more beneficial to focus on enhancing airflow in the dehydrator than increasing temperature. Increased airflow can be achieved through addition of a fan or by having a controlled vent system.

6.2.1 Fan

Our original design proposal from last semester was an active solar dehydrator, which included a solar panel to power a fan. The fan would be placed at the top of the solar collector and create a greater airflow into the drying chamber. Due to funding constraints, we did not purchase a solar panel and a fan. However, this would have been a good way to improve the drying conditions of our dehydrator and we believe it should be implemented in an optimized design.

6.2.2 Controlled Roof Ventilation

As an alternative to adding a fan, we propose a roof design with a controlled vent opening at the top. As illustrated in figure he roof would look the same as our current roof and sit at a 90 degree angle. One of the edges would sit firmly in place, while the other would be hinged to the top of the drying chamber. The hinge could be adjusted to open at any desirable angle to increase or decrease the vent opening. We decided on this roof system because as mentioned previously, ideal drying conditions are achieved with air flow that is laminar in the solar collector, turbulent in the drying chamber and laminar as it exits the dehydrator. The air will naturally want to flow out the top of the drying chamber and therefore we think it is best to have the vents be placed on the roof rather than the sides of the drying chamber. The hinged piece of wood will have an L-shaped metal beam placed on top that will prevent water from entering the structure when it is raining.

Figure 11. Isometric view of the hinged roof.

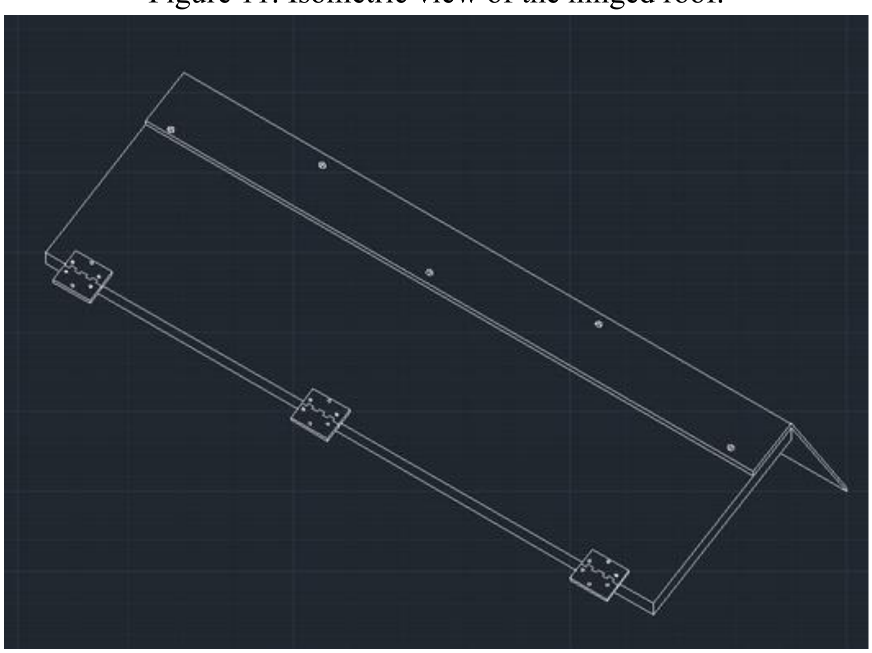

Figure 12. a) Front view of the hinged roof b) Side view of the hinged roof

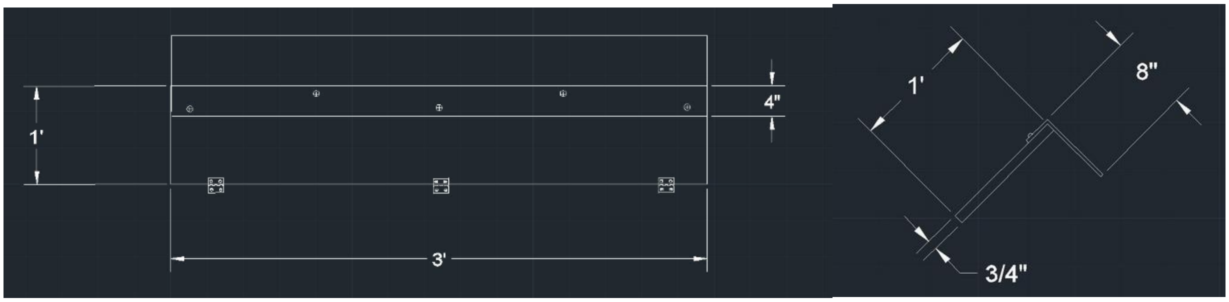

The hinged roof system is illustrated in figures 11 and 12 above.

To add further optimization and complexity, the vent could be coupled with sensors within the dehydrator to create an automated vent system. Sensors for temperature, air speed and relative humidity would take readings from inside the dehydrator and would control the size of the vent opening. This system could have multiple settings for optimal drying conditions of different herbs in order to provide further quality assurance.

7. CONCLUSION

The goal of our project was to design an herb dehydrator for MSEG that has a higher capacity and can be located on the farm. Due to these criteria, we designed a solar herb dehydrator that relies on passive heating. The design was modeled using COMSOL to determine an approximate airflow within our dehydrator. The structure of the prototype was constructed out of wood and the solar collector was constructed with plexiglass and carbon steel. The prototype was tested using a Velocicalc to measure air velocity and temperature probes to measure the change in temperature within the drying chamber over time. However, air velocity was unable to be measured during testing. More data has to be collected under more ideal conditions to properly assess its performance. The optimization of our design includes moving the location of the wheels and the addition of either a fan or a controlled roof for ventilation.

Solar drying can be successfully implemented in places where sunlight is abundant. It can particularly be used in developing countries because its design and implementation is relatively cheap and easy. It is a very economic way of drying compared to conventional drying methods. Moreover, it is an environmentally friendly drying method for it does not rely on fossil fuels. In this particular design we focused on the drying of herbs, however, this method can be applied to the drying of fruits and vegetables as well.

We will be entering our design in the “Gunlogson Student Environmental Design Competition”. The competition is to encourage undergraduate students to participate in the design of a relevant engineering project and to provide an arena of professional competition for environmentally and biologically related design projects. We will submit our report to this competition one week after the due date of our final design report, which will be April 21st, at 11:00PM EST.

8. REFERENCES

Akarslan, F. 2012. Solar-Energy Drying Systems, Modeling and Optimization of Renewable Energy Systems. ISBN: 978-953-51-0600-5, InTech, Available from: http://www.intechopen.com/books/modeling-and-optimization-of-renewable-energy-systems/solar-energydrying-systems-and-applications. Accessed on 29 March 2015.

Akpinar, E. K. 2011. Drying of Parsley Leaves in a Solar Dryer and Under Open Sun: Modeling Energy and Exergy Aspects. Journal of Food Process Engineering. 32(1):27-48. DOI: 10.1111/j.1745-4530.2008.00335.x

Bena, B., Fuller, R.J., 2002. Natural convection solar dryer with biomass back-up heater. Solar Energy 72 (1), 75–83.

Blair, R., G. Calota, A. Crossman, F. Drake, K. O'Keefe. 2005. Design of a solar powered fruit and vegetable drier. Mechanical Engineering Undergraduate Capstone Projects. Paper 44. Available online: http://hdl.handle.net/2047/d10011730. Accessed 29 March 2015.

CFIA 2014, Food Safety Practices Guidance For Spice Manufacturers, Guidance Document Repository

Chen, H.-H., Hernandez, C.E., Huang, T.-C., 2005. A study of the drying effect on lemon slices using a closed-type solar dryer. Solar Energy 78, 97–103.

Condorı´, M., Saravia, L., 2003. Analytical model for the performance of the tunnel-type greenhouse drier. Renewable Energy 28, 467–485.

El-Sebaii, A.A., Aboul-Enein, S., Ramadan, M.R.I., El-Gohary, H.G., 2002. Experimental investigation of an indirect type natural convection solar dryer. Energy Conversion and Management 43, 2251–2266.

Emery, K.A. 1986. Solar Simulators and I-V Measurement Methods. Solar Energy Research Institute, Golden Colorado. Device Performance: 251-260.

Ekechukwu, O.V., B. Norton. 1999. Review of solar-energy drying systems III: low temperature air-heating solar collectors for crop drying applications. Energy Conversion and Management. 40(6): 657-667. doi:10.1016/S0196-8904(98)00094-6

Fodor, E. 2006. Build a Solar Food Dehydrator. Mother Earth News.

Forson, F.K, Nazha, M.A.A., Rajakaruna, H., 2007. Modelling and experimental studies on a mixed-mode natural convection solar cropdryer. Solar Energy 81, 346–357

Government of Canada. Daily data report Sainte-Anne-De-Bellevue. Available online: http://climate.weather.gc.ca/climateData/dailydata_e.html?timeframe=2&Prov=QC&StationID=10873&hlyRange=1994-02-01%7C2015-03-29&cmdB1=Go&cmdB2=Go&Year=2014&Month=9&cmdB2=Go# Accessed 1 April. 2015.

Hii, C.L., S.V. Jangam, S.P Ong, A.S. Mujumdar. 2012. Solar Drying: Fundamentals, Applications, and Innovations. ISBN: 978-981-07-3336-0.

Hossain, M.A., Bala, B.K., 2007. Drying of hot chilli using solar tunnel drier. Solar Energy 81, 85–92.

Inglehart, J.A. Aluminum vs. Steel Conductivity. Available online: http://www.ehow.com/facts_5997828_aluminum-vs_-steel-conductivity.html. Accessed 12 April 2015.

Ivanova, D., Enimanev, K., Andonov, K., 2003. Energy and economic effectiveness of a fruit and vegetable dryer. Energy Conversion and Management 44, 763–769.

Khoshmanesh, S. 2006. Design of solar dehydrator, coupled with energy storage in rock bed reservoir for fish drying process.

Komp, R. 2005. Food and Herb Dryer From Maine Solar Primer. Build it Solar.
Reynolds, S., P. Williams. 2006. So Easy to Preserve. Bulletin 989. Cooperative Extension Service, University of Georgia.

Mazria, Edward, (1979), The Passive Solar Energy Book: A Complete Guide to Passive Solar Home, Greenhouse, and Building Design. Emmaus, PA: Rodale,

Müller J. 2007. Convective drying of medicinal, aromatic and spice plants: a review. Stewart Postharvest Review, 4:2.

Müller J. Argyropoulos D. 2011. Effect of convective drying on quality of lemon balm (*Melissa officinalis* L.) Procedia Food Science 1: 1932-1939.

Pangavhane, D.R., Sawhney, R.L., Sarsavadia, P.N., 2002. Design, development and performance testing of a new natural convection solar dryer. Energy 27, 579–590.

Pidwirny, M. 2006. Earth-Sun Relationships and Insolation. Fundamentals of Physical Geography 2. [Accessed April 10th, 2015] http://www.physicalgeography.net/fundamentals/6i.html

Raghavan, V. 2015. Solar Drying. Lecture notes of Post-Harvest Drying. McGill University.

Scanlin, D., M. Renner, D. Domermuth, H. Moody. 1999. Improving Solar Food Dryers. HomePower Magazine. 69: 24-34.

Simate, I.N., 2003. Optimization of mixed-mode and indirect-mode natural convection solar dryers. Renewable Energy 28, 435–453.

Weiss, W., J. Buchinger. 2012. Solar Drying. Available online: http://www.aee-intec.at/0uploads/dateien553.pdf

9. APPENDICES
APPENDIX 1- Charts and Graphs

Figure 1. Psychrometric chart

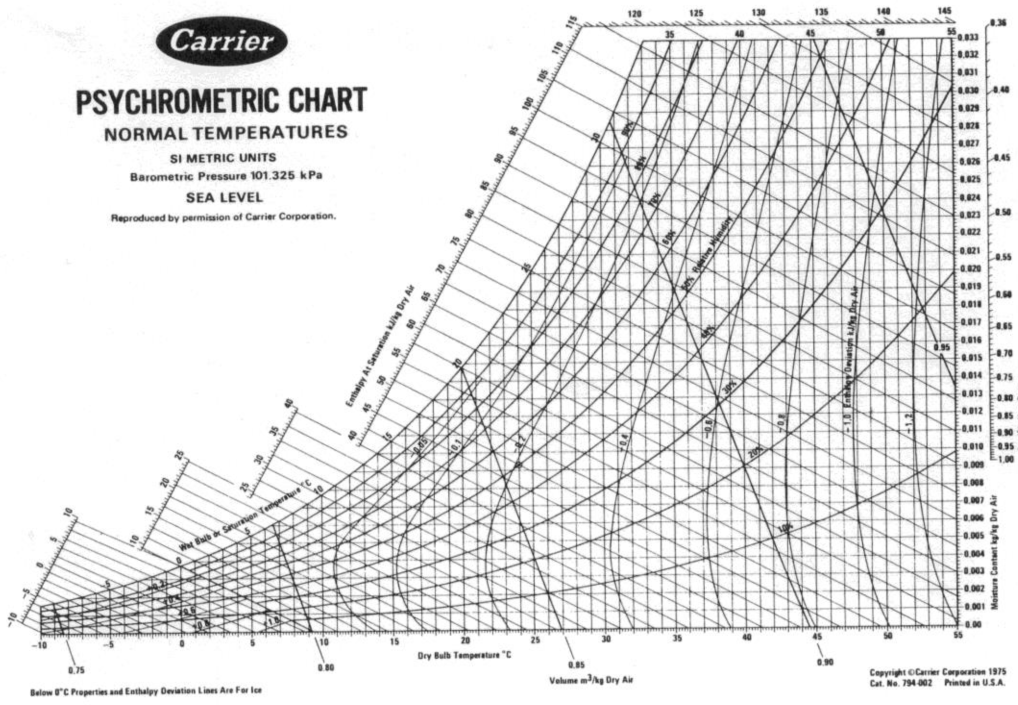

Figure 2. Monthly values of available insolation (Pidwirny, 2006).

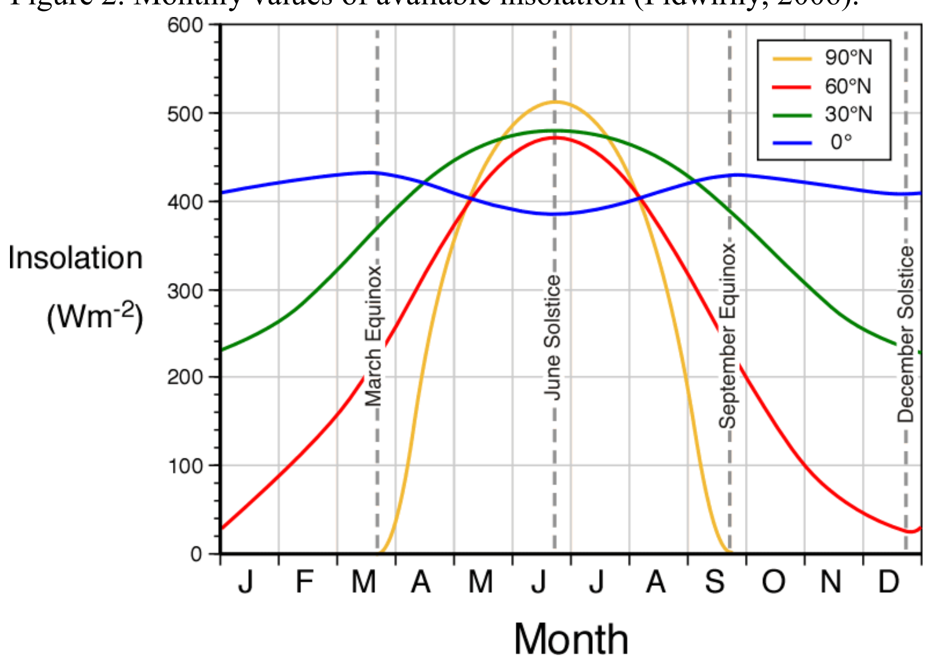

Figure 3. Solar elevation and solar azimuth throughout the day from June to December, specifically for Sainte-Anne-de-Bellevue at latitude of 45.41 degrees.

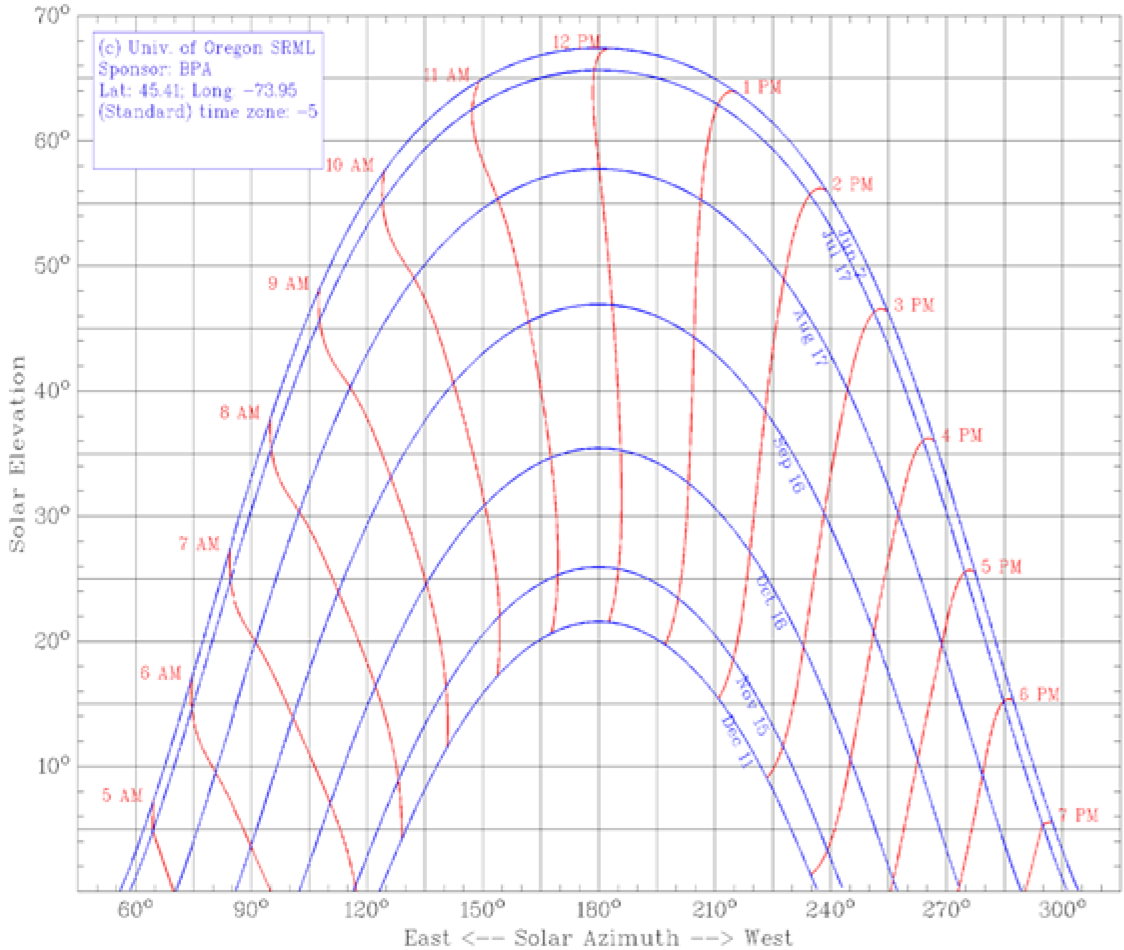

APPENDIX 2- Tables

Table 1. Optimal commercial drying temperatures for various herbs.

Common Name	Latin Name	Optimal Temperature	Essential Oil Loss	Reference
Lemon Balm	Melissa officinalis	40°C	<20%	Müller & Argyropoulos, 2007
Peppermint	Mentha x piperita	30°C	0%	Müller, 2007
Basil	Ocimum basilicum	30°C	0%	Müller, 2007
Sage	Salvia officinalis	40°C	0%	Müller, 2007
Chamomile	Chamomilla recutita	40°C	12%	Müller, 2007

Table 2. Weather Data for Sainte-Anne-De-Bellevue (Government of Canada, ND).

Month	Mean temperature (°C)	Average maximum temperature (°C)	Average minimum temperature (°C)	Rainfall (mm)	Extreme windspeed (km/h)
June	19.4	24.7	13.9	142.7	43
July	20.5	25.0	16.0	77.7	67
August	19.6	24.6	14.6	60.9	44
September	15.4	20.9	9.7	50	61

Table 3. Temperature data from testing the prototype.

Time (minutes)	Temperature (Celcius)			
	ambient	inside left	inside right	on aluminum
0	22	22.3	22	
5	21.4	22.6	22.5	
10	20.9	22.7	22.3	
15	16.4	20.9	20.9	24.9
20	19.3	22.6	22.2	25.4
25	20.4	22.9	22.3	25.6
30	20.4	25.2	24.1	26.4
32	20.7	25.5	24.4	26.6
34	20.8	25.9	24.4	26.8

37	20.7	26	24.6	27
42	20.4	26.2	24.7	27.2
48	20.5	26.3	24.6	27.2
51	20.4	26.3	24.3	27.2
53	19.7	26.3	24.4	27.5
56	20.3	26.5	24.3	27.4
60	20.3	26.6	24.3	27.3
63	19.8	26.6	24.5	27.8
67	20.2	26.6	24.6	27.6
73	19.9	26.8	24.3	27.7
76	19.6	26.7	24.3	27.6
84	20.2	26.9	24.4	27.8

Table 4. Cost Breakdown of Prototype

Material	Price per unit	# units	Total price	Source
Wheels	32.99	2	65.98	Canadian Tire
Aluminum foil	2.49	2	4.98	Canadian Tire
Silicon sealing glue	3.99	1	3.99	Canadian Tire
Axial hinges	3.99	2	7.98	Canadian Tire
Wood Varnish paint	7.99	1	7.99	Canadian Tire
High temperature spray paint	6.99	1	6.99	Canadian Tire
Tax			15.26	Canadian Tire
High temperature black paint	8.99	1	8.99	Rona
Tax			4.94	Rona
Total cost of our construction			127.1	
Additional Materials				
1x2 beams	5	5	25	Rona
Stainless steel mesh	45	1	45	Rona
Acrylic Panel	30	2	60	Rona
Plywood	42	2	84	Reno Depot
Total cost with additional materials			341.1	